SILVER THICK FILM CONTACT FORMATION ON LOWLY DOPED PHOSPHOROUS EMITTERS

Gunnar Schubert[1], Jörg Horzel[2], Radovan Kopecek[1], Frank Huster[1] and Peter Fath[1]
[1]University of Konstanz, Department of Physics, P.O.Box X916, D-78457 Konstanz, Germany
p: +49-7531-88-2088, f: +49-7531-88-3644, gunnar.schubert@uni-konstanz.de,
[2]RWE SCHOTT Solar, Carl-Zeiss-Str, 63755 Alzenau, Germany, p: +49-6023-91-1735, joerg.horzel@rweschottsolar.com

ABSTRACT: In this contribution we study the potential of silver thick film metallization to contact weakly doped emitters with high sheet resistance values and low phosphorous surface concentrations. The influence of the phosphorous surface concentration on both, the electrical properties of the silver thick film contact and the contact formation processes is investigated. In order to study the contact formation processes we focused on the growth of silver crystals onto the silicon surface. It is shown that the crystal growth depends mainly on the excess phosphorous in the surface near emitter region. The sheet resistance is not the key parameter. The dependency on the electrical phosphorous surface concentration is less pronounced. Increased peak firing temperatures result in enhanced size and number of crystals grown on all investigated emitters. The silver growth on <111> oriented silicon surfaces starts at lower temperatures than on <100> oriented Si. It is shown that direct contacting of the crystals with conductive silver leads to specific contact resistances of $\rho_C < 10\ m\Omega cm^2$ on emitters with a surface concentration of $N_{D,surface} \approx 4 \cdot 10^{19}\ cm^{-3}$.
Keywords: silicon solar cell, thick film metallization, front contact

1 INTRODUCTION

Easy contacting of "high efficiency emitters" with high sheet resistances (>100 Ω/sq.) and low phosphorous surface concentrations in the range of $N_D=(1\text{-}5) \cdot 10^{19}\ cm^{-3}$ is one of the main tasks in developing highly efficient industrial silicon solar cells. Today the predominant contacting technique in the PV industry is silver thick film metallization. However, 40-60 Ω/sq. emitters with high surface concentrations, exceeding the solubility limit of phosphorus in silicon, are currently necessary to establish an ohmic contact to the n-type region of the solar cell. The high phosphorous surface concentration in these emitters leads to recombination losses that in turn lead to current and voltage losses.

Recently, several successful attempts were reported to contact emitters with sheet resistances up to 100 Ω/sq. with silver thick film pastes [1]. It was also reported that the surface texture influences the contact resistance on emitters with high sheet resistances [2]. In both papers diffusion drive-in steps were not reported therefore a P surface concentration well above $10^{20}\ cm^{-3}$ can be assumed. In this contribution we study the potential of silver thick film metallization to contact weakly doped emitters. The influence of the P surface concentration on both, the electrical properties of the silver thick film contact and the contact formation processes is investigated. The results are compared to the recently presented microscopic model of electrical contact formation [3].

Microstructure investigations of Ag thick film contacts showed that a glass layer accumulates at the silicon surface. It separates the bulk of the thick film finger from Ag crystals that were found to have grown on the silicon [1, 4, 5, 6]. The microscopic model of electrical contact formation identified Pb, in form of PbO_x in the glass frit, as the transport medium for silver to grow onto silicon [3]. Hilali et al. [1] assumed the crystal growth to be dependent on the P concentration in the emitter. On highly doped, <100> oriented emitters (R_{sheet} = 35 Ohm/sq., $N_D \approx 2 \cdot 10^{20}\ cm^{-3}$) the contact resistivity between silicon and silver crystal was measured to be in the range of 0.2 μOhmcm² [4]. Therefore the silver crystals grown onto the silicon seem to be indispensable to establish a current transport path from the emitter into the bulk of the thick film contact. The dominating current transport mechanism from the crystals to the finger bulk is, however, not identified yet.

Decreasing the P surface concentration is expected to lead to higher contact resistivities between silicon and the silver crystals. Following the calculations Schroder et al. [7] the contact resistivity between ideal silver - silicon contacts is around 1 mΩcm² for $N_D = 5 \cdot 10^{19}\ cm^{-3}$ and a barrier height of 0.78 eV. Therefore, number and size of the silver crystals grown onto the emitter are assumed to be even more important for the macroscopic contact resistance in case of lowly doped emitters. The main focus in this investigation is consequently on the influence of the phosphorous concentration on the silver growth on silicon.

2 SAMPLE PREPARATION

In this study we used simple solar cell structures with emitters differing in the phosphorous surface concentration. To exclude shunting or damaging of the space charge region by the metallization paste we used drive–in steps in order to obtain deep profiles for the emitter P concentration.

Four $POCl_3$ pre-deposition steps (820°C low $POCl_3$ flow; 820°C high $POCl_3$ flow; 860°C; 950°C) were performed on <100> oriented, 12.5x12.5 cm² semi-square Cz silicon (thickness: 330 μm, ρ = 1.5 Ωcm) after saw damage etching (NaOH, 80°C) and cleaning. After P-glass etching the wafers were divided in a reference and a "drive-in" group. Wafers belonging to the latter group were used to fabricate deep emitters with varying phosphorous surface concentrations by performing a drive-in diffusion at 950°C for 240 min in N_2 atmosphere to avoid pile-up effects. PECVD-SiN_x was deposited and the wafers were cut into to 5x5 cm² samples. Then front contacts were screen-printed using a commercial available, leaded Ag paste, optimised for 40 – 60 Ω/sq. emitters with high P surface concentrations. After printing the Al back contact, the samples were fired in an RTP-furnace (Steag AST SHS 100) to ensure an accurate

control of the process parameters. The peak firing temperature was varied in the range of $T_{peak, optimal}$ - 25K to $T_{peak, optimal}$ + 50K. Due to the statistical nature of the contact formation processes three samples per firing parameter and emitter were processed.

The pyrometer of the RTP furnace was calibrated carefully using two of the samples with 11 Ω/sq. and 83 Ω/sq. emitter. A Pt/Pt10%Rh thermocouple was bonded on the emitter side and the wafers were fired facing the pyrometer. The absolute temperature accuracy of the calibration was < 2%. The relative accuracy of subsequent firing cycles was measured to be < 1%. The firing parameters, serving as a starting point for the contact formation investigations, were found by optimising the process for 12.5x12.5 cm^2 mc Si industrial solar cell structures with 50 Ω/sq. emitters, SiN_x-ARC and NaOH etched surfaces applying the same metallisation pastes. These parameters resulted in fill factors above 77% (best cell: FF: 78.1%, V_{oc}: 617.7 mV).

3 SOLAR CELL CHARACTERISATION

3.1 Emitter characterisation

The fabricated emitters were characterised after P-glass etching by sheet resistance measurements (four point probe setup) and electrochemical capacitance voltage (ECV) measurement. The results are summarized in Figure 1. The variation of R_{sh} of emitter 4 after drive-in even on one wafer was quite high which might be due to an inhomogenous diffusion due to the low $POCl_3$ flow. The electrical active P concentration was determined by ECV measurements on one wafer of each group. The reference emitters showed a ≈ 12 – 400 nm deep plateau at $N_D = 1 - 3 \cdot 10^{20}$ cm^{-3}. Following e.g. Fair et al. [8] the chemically P concentration in the plateau is expected to be a factor 1.2 to 2 higher. After drive-in, the resulting profiles of emitter 1 and 2 show similar electrical active surface concentrations but a Gaussian shape, indicating a lower chemical surface concentration, because no P-source was present during the drive-in step. Emitter 3 and 4 show Gaussian shapes, too, with P surface concentrations of $N_D \approx 4 \cdot 10^{19}$ cm^{-3} and $N_D \approx 3 \cdot 10^{19}$ cm^{-3}, respectively. For these emitters it can be assumed that the chemical and the electrical P concentration depth profiles are identical with the electrically active P profiles.

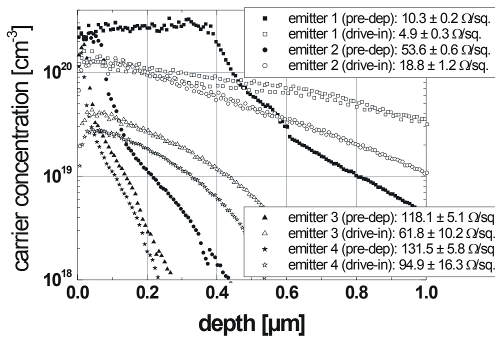

Figure 1: R_{sheet} (mean values of three samples) and electrical active P concentration as a function of depth of the 8 studied emitters.

3.2 Cell parameters

The solar cells were characterized by IV-measurements to determine the global cell parameters, ILIT (Illuminated Lock-In Thermography) to identify shunts and TLM (transfer length method) measurements to determine the contact resistance. In Figure 2 the fill factors (average over three cells) and specific contact resistances (average over 19 fingers of one cell per group) of the "drive-in emitter" cells are presented. Apart from the cells with the highly doped drive-in emitter 1, all samples show very low fill factors due to very high contact resistivities. The contact resistivities of emitter 2-4 are difficult to measure and scatter, so that the values given in Figure 2 are only approximate.

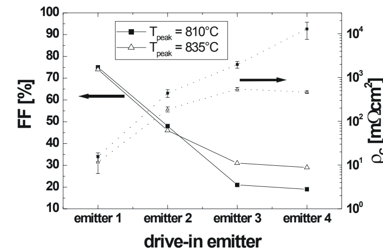

Figure 2: FF and ρ_C of "drive-in emitter" cells

Dark IV analysis and ILIT measurements revealed that the "drive-in emitter" cells are not shunted. Although difficult to extract due to the high series resistance, even drive-in emitter 4 – cells showed shunt values of $R_{shunt} > 1000$ Ωcm^2.

4 CONTACT FORMATION

The contact formation was investigated by SEM and EDX analysis using the TLM samples. Cross-section investigations of the contact show only limited parts of the finger. To account for the statistical nature of the contact formation process we therefore set our focus on the analysis of the silicon surface below the silver finger. The silver grid was removed by dipping the samples in diluted HF (2%) for 3 min. This etching procedure guarantees that only the glass layer and the bulk of the silver finger fall off, whereas the silver crystals grown onto the silicon are not affected. 5-10 fingers distributed over an area of 2.5 x 2.5 cm^2 selected from each solar cell were analysed at randomly chosen positions.

All analysed samples show silver crystal clusters located at the edge regions of the fingers. From Figure 3 it can be deduced that these clusters are the residues of the sintered paste. In these areas a higher glass to silver ratio is likely, however, it is not completely understood why the residues do not fall off during HF dipping.

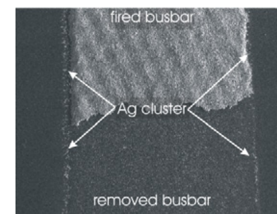

Figure 3: Partly removed busbar on n-Si, $N_D = 6 \cdot 10^{19} cm^{-3}$. Ag clusters are located at the edge regions.

4.1 Crystal growth vs. doping concentration

First we investigated the crystal growth in dependence of the P surface concentration at the optimal peak firing temperature (810°C). In Figure 4 a selection of representative SEM pictures is presented. The number and size of the grown crystals is greatest on reference emitter 1 and 2 (size around 500 nm). On all “drive-in” emitters less and smaller crystals have grown (size ≈ 200-300 nm). The differences in Ag crystal growth on those emitters are little. On reference emitter 3 and 4 the crystal growth is comparable to the growth on the corresponding drive-in emitters.

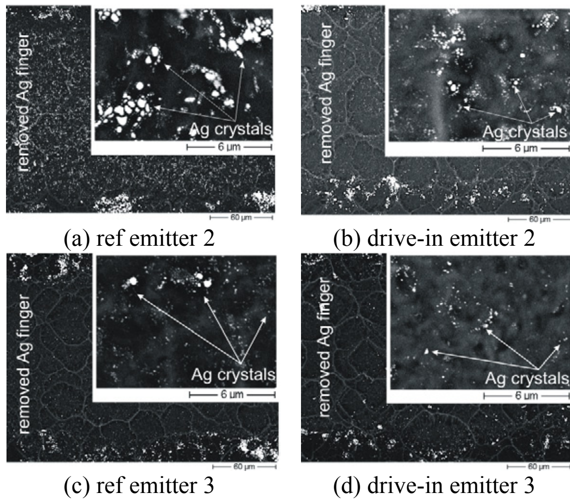

(a) ref emitter 2 (b) drive-in emitter 2

(c) ref emitter 3 (d) drive-in emitter 3

Figure 4: Dependency of crystal growth on the P surface concentration at the optimal peak firing temperature.

It can be concluded that crystal growth depends mainly on the excess phosphorous at the surface. The sheet resistance is not the key parameter. The minor differences between reference emitter 3 and 4 and the corresponding drive-in emitters can be explained by the glass frit etching into the silicon. As the highly doped plateau is only 10 – 15 nm deep for these emitters, it is likely that the effective P surface concentration for silver crystal growth is lower ($< 1\cdot 10^{20}\ cm^{-3}$). Following the contact formation model in [3] the activation energy of the liquid Ag-Pb melt with silicon can be assumed to be lower in the case of highly doped emitters, i.e. crystal growth at a constant peak firing temperature is less effective in case of emitters with lower excess phosphorous at the surface.

4.2 Crystal growth vs. peak temperature

Increasing the peak firing temperature leads to the growth of more and larger Ag crystals on all emitters. The difference in crystal growth between reference and drive-in emitters gets smaller (see Figure 5). At high peak temperatures the differences in crystal growth due to the phosphorous surface concentration vanish. Although the peak temperature in this experiment exceeds the Ag-Si eutectic (840°C [9]), it is likely that the crystal growth is still via a liquid Pb-Ag melt. Experiments presented in [3] indicate that temperatures near the melting point of Ag and/or longer peak firing times are necessary to grow Ag crystals on Si via an Ag-Si eutectic reaction.

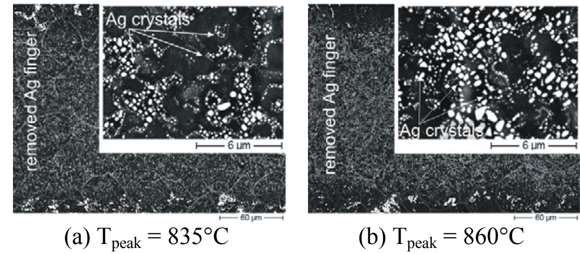

(a) T_{peak} = 835°C (b) T_{peak} = 860°C

Figure 5: Crystal growth on drive-in emitter 3. (a) T=835°C (size≈350 nm) (b) T=860°C (size≈450 nm)

4.3 Influence of surface texture

Recently it was reported that the surface texture influences the contact resistance on emitters with high sheet resistances [6]. Our experiments on drive-in emitters with $N_S \approx 5\cdot 10^{19}\ cm^{-3}$ comparing iso-textured and NaOH etched mc Si industrial solar cells showed higher fill factors on the iso-textured cells (FF=64%) than on the NaOH etched surfaces (FF=34%).

To test the influence of the surface texture on the crystal growth, polished, <100> oriented n-type wafers with a bulk doping of $N_D = 6\cdot 10^{19} cm^{-3}$ (measured with ECV) were used to exclude differences in the diffusion profile due to texturing. Half of the wafers were alkaline-etched to obtain a pyramidal surface with <111> oriented surface planes. After printing the front grid using the same Ag paste as in the previous experiments the samples were fired in the RTP furnace at fill factor optimized parameters varying the peak temperature. SEM and EDX analysis was performed after removal of the fingers in diluted HF (2%) for 6 min. In Figure 6 representative SEM pictures are presented. The crystals start to grow on the side surfaces of the pyramids at lower temperatures compared to the <100> oriented surface.

This experiment indicates that the Ag crystal growth depends besides temperature and P concentration on the orientation of the silicon. The activation energy for Ag crystals to grow on <111> oriented surfaces is supposed to be lower in comparison to the energy required to start growing on <100> Si surfaces. Additionally, on textured surfaces the probability of the appearance of quasi-direct crystal-finger interconnections is increased (Figure 7).

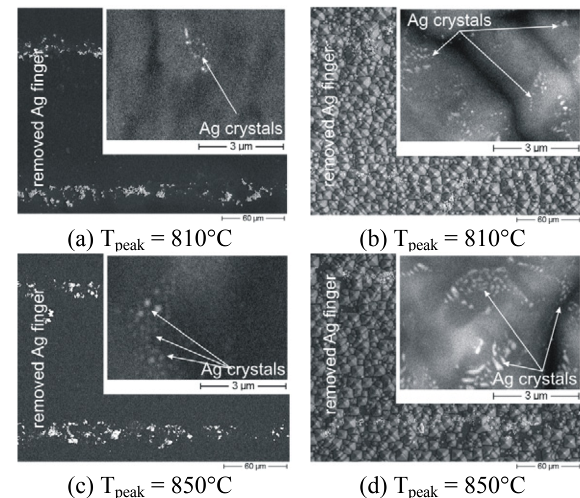

(a) T_{peak} = 810°C (b) T_{peak} = 810°C

(c) T_{peak} = 850°C (d) T_{peak} = 850°C

Figure 6: Ag crystal growth on polished <100> Si surfaces and on alkaline textured Si surfaces with $N_{D,surface}=6\cdot 10^{19} cm^{-3}$ at different peak firing temperatures.

Figure 7: Cross section of lead free Ag paste on alkaline textured <100> Cz Si surface, 50 Ω/sq. emitter.

4.4 Electrical properties

To test the electrical properties of the emitter – crystal contact the silver ink fingers of the TLM test structures were removed in diluted HF. The remaining Ag crystals grown onto the emitter were selectively contacted by conductive silver. A drying step at 50°C for 1 min was performed and the contact resistance was measured using the TLM measurement setup. The contact width was assumed to be same as the original finger width after firing. To test the selectivity of this contacting method conductive Ag was applied on the bare "drive-in" emitter 1 after etching off the Ag crystals in NH_3:H_2O_2 (1:1) followed by an HF-dip. SEM analysis revealed that all crystals were removed.

In Figure 7 the results are summarized. Although size and number of the Ag crystals increase, firing at higher peak temperatures reduces the number of quasi-direct interconnections due to the increased glass layer thickness [5]. The contact resistivity decreases drastically when contacting the Ag crystals directly. The contacts to drive-in emitter 1, 2 and 3 are homogenous (log scale). As the sheet resistance of drive-in emitter 4 varies the contact resistivity scatters considerably. Contacting the bare drive-in emitter 1 with conductive Ag resulted in $\rho \approx 600$ mΩcm^2, proving the selectivity of this method.

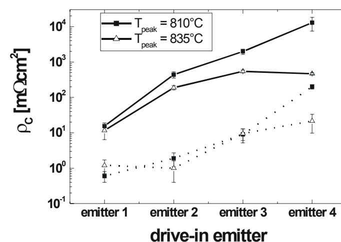

Figure 7: Contact resistivity of "drive-in emitter" cells (mean values) after firing (straight lines) and after direct contacting the Ag crystals (dotted lines).

It can be concluded that the most effective current transport path in a silver thick film finger is via quasi-direct crystal – finger contacts. It is surprising that no correlation between T_{peak} and the contact resistance of directly contacted fingers is found except for "drive-in" emitter 4. As shown in section 4.2 number and size of the Ag crystals depend on the firing temperature. Assuming that the current transport is only via Ag crystals one would expect a decreased contact resistance with increased area covered by the crystals. The result can be understood considering that the huge crystals grown at higher peak temperatures penetrate deeper into the silicon. Additionally the glass frit etches deeper into the emitter, too. It is likely that the effective crystal area contributing to the current transport significantly is less increased as the total crystal area. In addition it cannot be excluded that the Ag clusters bordering each finger independent of doping and temperature contribute to the current transport considerably. Nevertheless, this result has to be analysed carefully.

5 SUMMARY AND CONCLUSION

The results of the investigation of silver thick film contact formation on lowly doped emitters can be summarised as follows:

1. Ag crystal growth on silicon depends mainly on the excess chemical surface concentration, the peak firing temperature and the silicon orientation.
2. Contacting Ag crystals directly resulted in $\rho_C < 10$ mΩcm^2 on emitters with $N_D \approx 4 \cdot 10^{19}$ cm^{-3}.
3. No clear correlation between peak firing temperature and contact resistance of directly contacted silver-silicon contacts was found.

From these results it can be concluded that in principle contacting of "high efficiency" emitters with thick film silver inks is possible. Using the same paste and adapted firing parameters Ag crystals on lowly doped emitters can be grown similar to those grown on standard industrial emitters with standard firing parameters. Textured silicon wafers with a great fraction of <111> silicon side surfaces support the formation of silver-silicon contacts. The task for developing high efficiency silver inks is therefore to increase the current transport properties in the formed contact from the Ag crystals into the finger bulk. Two ways are possible: 1. by developing a glass frit, so that the activation energy for Ag crystal growth on moderately doped emitters is lowered. 2. by increasing the conductivity of the fired glass layer e.g. by reducing the glass layer thickness and/or by supporting a multi-step tunnelling mechanism through the glass after firing. Nevertheless further investigations are necessary to understand the role of the silver crystals for the current transport completely.

ACKNOWLEDGEMENTS

We would like to thank P. Karzel and E. Wefringhaus for processing and measurement support. The underlying projects of parts of this paper were supported with funding of the German BMU under contract number 0329844F (OPTIMAN) and by the EC under project No. ENK6-CT-2001-00560 (EC2Contact). The content of this publication is the responsibility of the authors.

REFERENCES

[1] M. Hilali et al, Proc. 19th EUPVSEC, Paris, (2004) 1300-1303

[2] A. v. d. Heide et al, Proc. 19th EUPVSEC, Paris, (2004) 701-704

[3] G. Schubert et al, Proc. 19th EUPVSEC, Paris, (2004) 813-816

[4] C. Ballif et al, Appl. Phys. Lett. 82, No. 12, (2003) 1878-1880

[5] C. Khadilkar et al, 14th PVSEC, Bangkok, (2004) in print

[6] G. Schubert et al, 14th PVSEC, Bangkok, (2004) in print

[7] D. K. Schroder and D. L. Meier, IEEE Trans. on Electron Devices, Vol. 31, No. 5, (1984) 637-647

[8] R.B. Fair et al., J. Electrochem. Soc., 124, No.7, (1977) 1107-1118

[9] T. B. Massalski, Binary Alloy Phase Diagrams, 2nd Edition, 1-3 (ASM International, USA, 1992)